第 30 卷第 9 期
2014 年 9 月

无 机 化 学 学 报
CHINESE JOURNAL OF INORGANIC CHEMISTRY

Vol.30 No.9
2141-2150

含 4,4′-联吡啶桥联的阳离子链和嘌呤–羧酸根抗衡阴离子的一维 Fe^{II}和 Co^{II}聚合物,及由混合羧酸根配体构筑的二维 Eu^{III}聚合物的合成与表征

周映霞*,[1] 王睿颖[2] 卢周卉[3] 储彩琴[4] 吴本来*,[4] 张鸿云[4]

([1]河南农业大学理学院,郑州 450002)

([2]河南化工职业学院,郑州 450042)

([3]北京林业大学园林学院,北京 100083)

([4]郑州大学化学与分子工程学院,郑州 450052)

摘要:通过 2′,3′-双脱氧肌苷和氯乙酸反应,得到 1 个多功能配体 2-(6-oxo-6,9-dihydro-1H-purin-1-yl)acetic acid (HL)。该配体与其它附加配体一起与相应的金属盐反应,分别得到 3 个配位聚合物{[Fe(4,4′-bpy)$(H_2O)_4$]$(L')_2$}$_n$ (**1**),{[Co(4,4′-bpy)$(H_2O)_4$] $(L')_2$}$_n$ (**2**)和{[Eu$(ox)_{0.5}$(su)$(H_2O)_2$]·H_2O}$_n$ (**3**)(4,4′-bpy=4,4′-二联吡啶,ox=草酸盐,su=琥珀酸盐,L′=L 的互变异构体 2-(6-oxo-6,7-dihydro-1*H*-purin-1-yl)acetate]。3 个配合物均为单斜晶系 *C*2/*c* 空间群。配合物 **1** 和 **2** 为异质同构体,是由 4,4′-二联吡啶桥联金属离子形成的一维链状结构,配合物 **3** 是由混合羧酸根构筑的二维框架结构。在配合物 **1** 和 **2** 中,脱质子的配体 HL 没有与金属离子配位,而是以互变异构体 L′并通过氢键结合成二聚阴离子对$[(L')]_2$作为抗衡离子存在于配合物中。在配合物 **3** 中,配体 HL 分解为草酸根,2 个 Eu^{III}被草酸根连接成二聚单元,这个二聚单元又被琥珀酸根连接成二维聚合物。另外还对配合物 **1** 和 **2** 的红外光谱、热分解性质以及配合物 3 的荧光性质进行了分析研究。

关键词:含嘌呤的羧酸配体;配位聚合物;晶体结构;热分析;荧光

中图分类号:O614.81$^+$1;O614.81$^+$2;O614.33$^+$8 **文献标识码**:A **文章编号**:1001-4861(2014)09-2141-10

DOI:10.11862/CJIC.2014.284

Syntheses and Determination of 1D Fe^{II} and Co^{II} Polymers Containing 4,4′-Bipyridine-Bridged Cationic Chain and Counterion Purine-Containing Carboxylate, and 2D Eu^{III} Polymer of Mixed Carboxylate Ligands

ZHOU Ying-Xia*,[1] WANG Rui-Ying[2] LU Zhou-Hui[3]

CHU Cai-Qin[4] WU Ben-Lai*,[4] ZHANG Hong-Yun[4]

([1]*College of Sciences, Henan Agricultural University, Zhengzhou* 450002)

([2]*Henan Vocational College of Chemical Technology, Zhengzhou* 450042)

([3]*School of Landscape Architecture, Beijing Forestry University, Beijing* 100083)

([4]*College of Chemistry and Molecular Engineering, Zhengzhou University, Zhengzhou* 450052)

Abstract: A purine-containing multifunctional ligand 2-(6-oxo-6,9-dihydro-1*H*-purin-1-yl)acetic acid (HL) was synthesized through the reaction of chloroacetic acid with 2′,3′-dideoxyinosine. Reactions of HL, corresponding metal salts and accessional ligands yield three new coordination polymers {[Fe(4,4′-bpy)$(H_2O)_4$]$(L')_2$}$_n$ (**1**), {[Co(4,4′-bpy)$(H_2O)_4$] $(L')_2$}$_n$ (**2**) 和 {[Eu$(ox)_{0.5}$(su)$(H_2O)_2$]·H_2O}$_n$ (**3**) (4,4′-bpy=4,4′-bipyridine, ox=oxalate, su=

收稿日期:2013-11-30。收修改稿日期:2014-03-30。

国家自然科学基金(No.20771094 和 21271157),结构化学国家重点实验室科学基金(No.20120008)资助项目。

*通讯联系人。E-mail:zhoulao@139.com,wbl@zzu.edu.cn

succinate, and L′=tautomer 2-(6-oxo-6,7-dihydro-1*H*-purin-1-yl)acetate), respectively. Complexes **1**~**3** all belong to the monoclinic system with a *C*2/*c* space group. Isostructural polymers **1** and **2** feature a 1D cationic chain bridged by 4,4′-bpy with metal nodes whereas polymer **3** is a 2D framework bridged by mixed carboxylate. In **1** and **2**, the ligands HL are not coordinated with metal ions, only as counter ions in a hydrogen-bonding cyclic dimer $[(L')]_2$. In **3**, ligands HL were decomposed into oxalic acids, and two $Eu^{Ⅲ}$ are connected together by the oxalate to form dimeric units which are further bridged into the novel 2D polymer by succinates. Otherwise, infrared spectra and thermal behaviors of **1** and **2** as well as the fluorescence of **3** were also investigated. CCDC: 917893, **1**; 91789, **2**; 917892, **3**.

Key words: purine-containing carboxylate ligand; coordination polymer; crystal structure; thermal analysis; fluorescence

Self-assembly through coordinate bonds and weakly intermolecular interactions has proven to be powerful tools for constructing specific configurations such as rings, cages, funicular hydrocarbons, polymers, and networks[1-2]. Recent decades of research show that among the factors which direct the self-assembly processes, the ligand plays a crucial role in deciding the structures of the metal complexes. Purine and its derivatives can be acted as probes in therapeutics to investigate biological systems and as spacers in supramolecular self-assembly to construct models for understanding many natural and synthetic systems[3-12]. This kind of bioactive N-heterocyclic compounds is endowed with multiple binding sites for the assembly of higher dimensional supermolecules through coordination, hydrogen-bonding, and π-π interactions[13-16]. The construction of purine-containing complexes is very significative of the investigation into the influence of metal ions on the structures and functions of resulting assemblies. Currently, carboxylic acids, especially N-donor aromatic acids, have attracted interest in construction of metal-organic frameworks due to the diversity coordination modes and hydrogen bonds originating from carboxyl groups[3,17-18]. N-donor aromatic carboxylates have been widely investigated as good reactants in the construction of inorganic-organic hybrid materials[19-21]. The multiple coordination modes of carboxylate groups and N atoms lead to functional characteristics and colorful geometry chemistry of metal-organic frameworks[22]. Especially, the obvious distortion of carboxyl from the conjugated heterocycle can provide a special configuration to make the construction of metal-organic helical polymers easier, which is very important in crystal engineering to obtain higher-dimensional helical complexes[23]. As our continuous work to extend the relevant structural types and establish synthetic strategies which could control dimensionality of the complexes, and finally to lead to desired organic-inorganic frameworks, in this paper, a purine-containing multifunctional carboxylate ligand, 2-(6-oxo-6,9-dihydro-1*H*-purin-1-yl)acetic acid (HL), and three new coordination polymers $\{[Fe(4,4'\text{-bpy})(H_2O)_4](L')_2\}_n$ (**1**), $\{[Co(4,4'\text{-bpy})(H_2O)_4]\ (L')_2\}_n$ (**2**) and $\{[Eu(ox)_{0.5}(su)(H_2O)_2]\cdot H_2O\}_n$ (**3**) were synthesized and characterized by elemental analysis, IR spectroscopy, ^{1}H NMR spectrum, X-ray single crystallography, thermal analysis and luminescence spectrum, respectively (4,4′-bpy=4,4′-bipyridine, ox=oxalate, and su=succinate). Alluringly, the synthesized ligand 2-(6-oxo-6,9-dihydro-1H-purin-1-yl)acetic acid in complex **1** and **2** show interesting tautomerization, and transformed into its tautomer 2-(6-oxo-6,7-dihydro-1*H*-purin-1-yl) acetate (L′) which cocrystallized with bpy-bridged 1D cationic chains as counterions (Scheme 1).

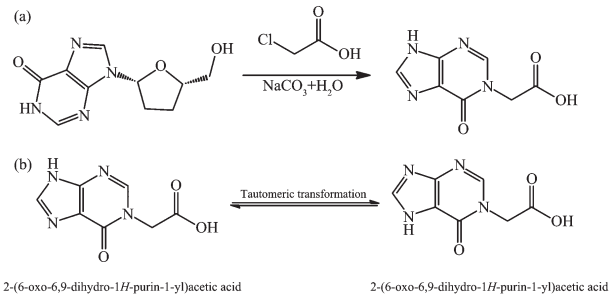

Scheme 1 Synthesis of ligand HL (a), and tautomeric transformation between HL and HL′ (b)

1 Experimental

1.1 Materials and physical measurements

All chemicals purchased were of reagent grade or better and were used without purification. IR spectra (KBr pellets) were recorded on a Nicolet NEXUS 470 FT-IR spectrophotometer from 400 to 4 000 cm^{-1}. Elemental analyses for C, H and N were performed with a Carlo-Erba 1106 elemental analyzer. ^1H NMR spectrum was recorded on a Bruker DPX-300 spectrometer at 300 MHz. Thermal analysis curves were scanned from 30 to 650 ℃ under atmospheres on a STA 409 PC thermal analyzer. The luminescence (excitation and emission) spectra for powdered samples were determined with Hitachi F-4500 spectrophotometer at room temperature with excitation wavelength of 393 nm, delay time of 0.01 ms, scan speed of 1 000 $nm \cdot s^{-1}$, excitation and emission slit width of 0.5 nm, voltage of 700 V, and test range of 350~700 nm.

1.2 Syntheses

1.2.1 Synthesis of 2-(6-oxo-6*H*-purin-1(9*H*)-yl)acetic acid (HL)

The ligand HL fusing purine and carboxyl groups for supramolecular assembly was synthesized according to the literature[3], and the white powder of HL was obtained with 68% yield based on dideoxyinosine. The pure product HL was fully determined by IR, ^1H NMR, and elemental analysis. Anal. Calcd. for $C_7H_6N_4O_3$ (%): C, 43.31; H, 3.11; N, 28.86. Found(%): C, 43.23; H, 3.06; N, 28.75. Selected IR data (KBr, ν / cm^{-1}): 3 429 (m), 3 132 (m), 2 961 (m), 1 684 (s), 1 575 (s), 1 544 (m), 1 390 (m), 1 230 (s), 1 195 (s), 955 (m), 838 (m), 788 (m), 643 (m), 535 (m). ^1H NMR (DMSO-d_6, 300 MHz) δ 3.35 (2H, CH_2), 7.97~8.10 (2H, $C_{(purin)}H$), 12.25 (1H, COOH), 13.32. (1H, $N_{(imidazole)}H$).

1.2.2 Synthesis of $\{[Fe(4,4'\text{-bpy})(H_2O)_4](L')_2\}_n$ (**1**)

A solution of $FeSO_4 \cdot 7H_2O$ (13.9 mg, 0.05 mmol) in water (2 mL) was added dropwise to a solution of HL (1.94 mg, 0.1 mmol) and 4, 4′-bipyridine (7.8 mg, 0.05 mmol) in methanol (10 mL) with stirring. The resulting mixture was stirred for a half-hour and filtered. Allowed the filtrate to slowly evaporate at room temperature for a week, brown square block crystals of **1** were obtained. Yield: 62% (based on Fe). Selected IR data (KBr, ν / cm^{-1}): 3 421 (s), 3 140 (m), 2 924 (w), 1 690 (m), 1 602 (s), 1 534 (w), 1 508 (w), 1 383 (m), 1 317 (w), 1 125 (w), 1 111 (w), 1 064 (w), 790 (w), 725 (w).

1.2.3 Synthesis of $\{[Co(4,4'\text{-bpy})(H_2O)_4](L')_2\}_n$ (**2**)

According to the same synthesis procedure of **1**, compound **2** was prepared with replacement of $FeSO_4 \cdot 7H_2O$ with $Co(NO_3)_2 \cdot 6H_2O$. The orange-red prismatic crystals suitable for X-ray analysis were obtained with 52% yield (based on Co). Selected IR data (KBr, ν / cm^{-1}): 3 415 (m), 3 146 (m), 2 917 (w), 1 693 (m), 1 601 (s), 1 535 (m), 1 509 (m), 1 490 (w), 1 386 (s), 1 318 (m), 1 223 (w), 1 180 (w), 1 126 (w), 821 (w), 790 (m).

1.2.4 Synthesis of $\{[Eu(ox)_{0.5}(su)(H_2O)_2] \cdot H_2O\}_n$ (**3**)

Solution of $Eu(NO_3)_3 \cdot 6H_2O$ (6.80 mg, 0.02 mmol) and succinic acid (2.40 mg, 0.02 mmol) in H_2O (6 mL) was added dropwise to a solution of HL (3.90 mg, 0.02 mmol) dissolved in water (4 mL) while vigorously stirring, and the mixed solution was continuously stirred for 20 min, then sealed in a 15 mL Teflon-lined steel reactor after a drop of triethylamine was added to the solution. The steel reactor was heated in an oven at 120 ℃ for 86 h, and then cooled to room temperature. Colorless block crystals of **3** suitable for single-crystal X-ray diffraction analysis were obtained with 23% yield (based on Eu). Selected IR data (KBr, ν / cm^{-1}): 3 311 (m), 2 926 (w), 1 670 (w), 1 584 (s), 1 537 (s), 1 424 (s), 1 404 (s), 1 304 (s), 1 281 (w), 1 218 (w), 1 175 (w), 1 005 (m), 681 (m), 646 (w), 585 (w).

1.3 X-ray structure determination

Data collection was on a Bruker SMART APEX-Ⅱ X-ray CCD diffractometer at 291(2) K using graphite monochromated Mo $K\alpha$ radiation (λ=0.071 073 nm). The structures were solved by direct methods and refined by full-matrix least squares using SHELX-97[24]. The hydrogen atoms of N and O atoms were located from difference Fourier maps and included in the final refinement by using geometrical restrains, while the other hydrogen atom positions were generated geometrically and were allowed to ride on their parent atoms. Details of the crystal structure determinations of complexes **1**~**3** are listed in Table 1, and selected bond distances and angles are in Table 2.

CCDC: 917893, **1**; 91789, **2**; 917892, **3**.

Table 1 Crystal data and structure refinement for the polymers 1, 2 and 3

Complex	**1**	**2**	**3**
Formula	$C_{24}H_{26}N_{10}FeN_{10}O_{10}$	$C_{24}H_{26}CoN_{10}O_{10}$	$C_5H_{10}EuO_9$
Formula weight	670.40	673.48	366.09
Temperature / K	291(2)	291(2)	291(2)
Wavelength / nm	0.071 073	0.071 073	0.071 073
Crystal system	Monoclinic	Monoclinic	Monoclinic
Space group	*C*2/*c*	*C*2/*c*	*C*2/*c*
a / nm	1.640 6(4)	1.636 45(2)	1.529 11(3)
b / nm	1.242 1(4)	1.229 98(2)	1.028 42(2)
c / nm	1.377 1(3)	1.372 69(2)	1.234 69(3)
β / (°)	97.806(19)	97.614 0(10)	103.09 1(2)
V / nm^3	2.780 2(12)	2.738 59(7)	1.891 17(7)
Z	4	4	8
D_c / (g·cm^{-3})	1.602	1.633	2.572
F(000)	1 384	1 388	1 400
Limiting indices	$-17 \leqslant h \leqslant 19$, $-11 \leqslant k \leqslant 14$, $-16 \leqslant l \leqslant 12$	$-19 \leqslant h \leqslant 19$, $-14 \leqslant k \leqslant 10$, $-16 \leqslant l \leqslant 15$	$-18 \leqslant h \leqslant 18$, $-12 \leqslant k \leqslant 11$, $-14 \leqslant l \leqslant 14$
Goodness-of-fit on F^2	1.041	1.059	1.142
R_1	0.045 8	0.036 2	0.022 2
wR_2	0.105 6	0.093 5	0.052 5
Data / restraints / parameters	2 320 / 0 / 208	2 572 / 0 / 209	1 651 / 6 /154
$(\Delta\rho)_{max}$, $(\Delta\rho)_{min}$ / (e·nm^{-3})	515, −364	496, −224	567, −1 200

Table 2 Selected bond distances (nm) and bond angles (°) for polymers 1, 2 and 3

1		**2**		**3**	
Fe1-O1	0.212 7(2)	Co1-O2	0.209 41(16)	Eu1-O6^{i}	0.239 6(2)
Fe1-O^{i}	0.212 7(2)	Co1-O2^{i}	0.209 41(16)	Eu1-O8	0.240 2(3)
Fe1-O2^{i}	0.213 8(2)	Co1-O1	0.209 51(15)	Eu1-O1	0.241 8(3)
Fe1-O2	0.213 8(2)	Co1-O1^{i}	0.209 51(15)	Eu1-O2^{ii}	0.243 2(3)
Fe1-Ni	0.219 2(2)	Co1-N1^{i}	0.216 04(16)	Eu1-O4	0.244 7(3)
Fe1-N1	0.219 2(2)	Co1-N1	0.216 04(16)	Eu1-O5^{iii}	0.245 5(3)
O1^{i}-Fe1-O1	86.34(13)	O2^{i}-Co1-O2	86.85(9)	Eu1-O7	0.247 0(3)
O1-Fe1-O2	173.63(9)	O1^{i}-Co1-O2^{i}	173.47(6)	Eu1-O3	0.252 5(3)
O1^{i}-Fe1-O2^{i}	173.63(9)	O1^{i}-Co1-O2	86.68(6)	Eu1-O6^{iii}	0.265 5(3)
O1-Fe1-O2^{i}	87.31(9)	O1-Co1-O2^{i}	86.68(6)	O6^{i}-Eu1-O8	73.72(11)
O2-Fe1-O1^{i}	87.31(9)	O1-Co1-O2	173.47(6)	O6^{i}-Eu1-O1	151.37(11)
O2-Fe1-O2^{i}	99.04(12)	O1-Co1-O1^{i}	99.81(9)	O8-Eu1-O1	133.33(11)
O1^{i}-Fe1-N1^{i}	94.12(9)	N1^{i}-Co1-N1	171.03(10)	O6^{i}-Eu1-O2^{i}	136.88(10)
N1^{i}-Fe1-N1	170.22(14)	O2^{i}-Co1-N1	95.14(7)	O8-Eu1-O2^{i}	67.06(10)
O2-Fe1-N1	85.67(9)	O1^{i}-Co1-N1	85.89(6)	O1-Eu1-O2^{i}	66.62(10)

Symmetry code: **1** and **2**: ^{i} $-x+1$, y, $-z+1/2$; **3**: ^{i} x, $-y$, $z-1/2$; ^{ii} $-x$, $-y+1$, $-z$; ^{iii} $-x$, y, $-z+1/2$.

2　Results and discussion

2.1　Synthesis, and IR spectra of HL and polymers 1~3

Compounds **1** and **2** were prepared in the reaction systems without adding base for deprotonation, and their crystals were obtained through slow evaporation of the resulting water/methanol solutions for about a week. Complex **3** was hydrothermally synthesized with triethylamine for deprotonation in the reaction system where ligands oxalate were produced via the *in situ* decomposition reaction of ligands HL.

Free ligand HL and polymers **1**~**3** were all determined by IR. For free HL, the characteristic peak for vibration of C=O in the acylamino is at 1 684 cm^{-1}, and the characteristic vibrations of $N_{(imidazole)}$-H is at 3 132 cm^{-1}, and the characteristic peak for vibration of C-H from -CH_2 is at 2 961 cm^{-1}. The IR spectra of **1** and **2** are similar. Strong peak for the stretching vibration of O-H from H_2O is at 3 421 cm^{-1} for **1** and 3 415 cm^{-1} for **2**. The middling absorptions at 3 140 cm^{-1} for **1** and 3 146 cm^{-1} for **2** are ascribed to $N_{(imidazole)}$-H while doubly strong absorptions at 1 600~1 690 cm^{-1} for **1** and **2** indicate the vibration of C=O in the acylamino[25]. Strong absorptions at 1 534 and 1 383 cm^{-1} for **1** and at 1 538 and 1 386 cm^{-1} for **2** are due to $\nu_{as}(COO^-)$ and $\nu_s(COO^-)$ stretching vibrations, respectively. The IR spectrum of **3** is different from **1** and **2** because of the decomposition of HL. The middling absorption at 3 311 cm^{-1} is ascribed to the vibration of O-H from H_2O, and the absorption at 1 670 cm^{-1} is due to the vibration of C=O while the characteristic peak for vibration of C-O is at 1 218 cm^{-1} which indicates the existence of COO^-.

2.2　Description of the crystal structures of 1~3

2.2.1　Crystal structures of **1** and **2**

Complex **1** is a 1D chain and crystallizes in the monoclinic with *C*2/*c* space group. The coordination environment of $Fe^{Ⅱ}$ is shown in Fig.1. Selected bond lengths and angles are given in Table 2. The asymmetric unit contains one half of $Fe^{Ⅱ}$, one half of 4,4′-bpy molecule, two coordinated water molecules, and one uncoordinated deprotonated ligand (L′)$^-$. The coordination sphere around every $Fe^{Ⅱ}$ is a distorted octahedron constructed by two nitrogen atoms (N1, $N1^i$) from two 4,4′-bpy molecules and four oxygen atoms (O1, $O1^i$, O2, $O2^i$) from four coordinated water molecules, and the two nitrogen atoms are located at the axial sites of the octahedron with the four oxygen atoms perching in the equatorial plane. In polymer **1**, the axial and equatorial transition angle of N1-Fe1-$N1^i$, O1-Fe1-O2, and $O1^i$-Fe1-$O2^i$ are 170.23(14)°, 173.64(9)° and 173.64(9)°, respectively (Table 2). The four oxygen atoms (O1, $O1^i$, O2, $O2^i$) are not coplanar with Fe1-O1 =Fe1-$O1^i$ and Fe1-O2 =Fe1-$O2^i$ being 0.212 7(2) nm and 0.213 8(2) nm, respectively (Table 2). There is a *C*2 axis passing through along *b*-axial direction and equally dividing every coordination octahedron meanwhile there is a inversion center *i* locating at the molecular center of every 4,4′-bpy. The two pyridyl rings of each 4,4′-bpy is not coplanar with a dihedral angle of 18.2°. Each pair of adjacent $Fe^{Ⅱ}$ is bridged by 4,4′-bpy to form a 1D cationic chain running along the *a*-axial direction (Fig.2). In the synthesis of **1**, the used ligand HL transformed into its tautomer 2-(6-oxo-6,7-dihydro-1*H*-purin-1-yl)acetate

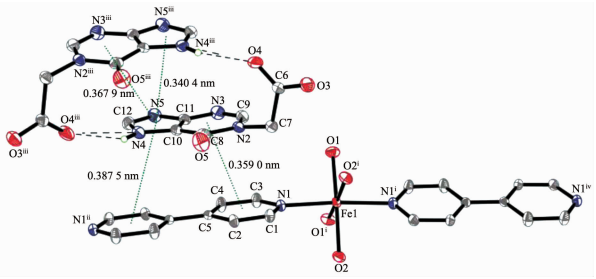

Counter ion of hydrogen-bonded cyclic dimer $[(L')]_2$ with partial hydrogen atoms are omitted for clarity; Symmetry code: [i] −*x*+1, *y*, −*z*+1/2; [ii] −*x*+3/2, −*y*+1/2, −*z*; [iii] 2−*x*, *y*, −*z*+1/2; [iv] *x*−1/2, −*y*+1/2, *z*+1/2

Fig.1　View of the coordination environment of the center $Fe^{Ⅱ}$ in **1** with thermal ellipsoids shown at 30% probability level

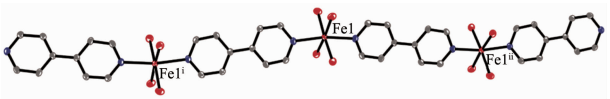

Hydrogen atoms are omitted for clarity; Symmetry code: [i] −*x*+3/2, −*y*+1/2, *z*; [ii] *x*−1/2, −*y*+1/2, *z*+1/2

Fig.2　Drawing of the 1D cationic chain in **1** with thermal ellipsoids shown at 30% probability level

(L′) through the rearrangement of the double bonds in the imidazole group of HL which decides the hydrogen atom riding on which $N_{imidazole}$, and two tautomer 2-(6-oxo-6,7-dihydro-1*H*-purin-1-yl)acetate are cyclized through $N_{imidazole}$–H ⋯ $O_{carboxylate}$ hydrogen-bonding to form a dimeric counter ion $[(L')^-]_2$ with a *C*2 axis passing through along *b*-axial direction (Fig. 1). In the dimeric counter ion $[(L')^-]_2$, there is stronger π-π stacking interaction between the imidazole rings (N4C10C11N5C12 and $N4^{iii}C10^{iii}C11^{iii}N5^{iii}C12^{iii}$) with a centroid-to-centroid distance being 0.340 4 nm and a dihedral angle being 9.3°, which obviously stabilized the dimeric conformation (Fig.1).

In the crystal structure of **1**, there is a complicated and interesting hydrogen-bonding network. In addition to two deprotonated uncoordinated HL′ connecting together by hydrogen bonds (N4–H4⋯$O4^{iii}$ 0.27 24(3) nm) to form a dimeric anion $[(L')^-]_2$, there are eight hydrogen bonds between the coordinated water molecules and every resulted dimeric anion $[(L')^-]_2$ with O_{water1}–H⋯$O_{carboxyl}$ being 0.273 8(3) nm, O_{water1}–H⋯$O_{carbonyl}$ being 0.272 9 (3) nm, O_{water2}–H⋯$O_{carboxyl}$ being 0.269 8(3) nm and O_{water2}–H⋯$N_{imidazole}$ being 0.279 9(4) nm (Table 3 and Fig.3). In this way, every dimeric anion $[(L')^-]_2$ connects with four cationic chains. Through those hydrogen-bonding interactions those 1D cationic chains and the dimeric anions $[(L')^-]_2$ assemble into a 3D supermolecule which is further stabilized through stronger π-π stacking interactions between pyridine rings C1C2C5C4C3N1 of the 4,4′-bpy from 1D chains and the purine rings N2C8C10C11N3C9 from the dimeric anions $[(L')^-]_2$ with a centroid-to-centroid distance of 0.359 0 nm (Fig.1, 4 and 5) and the dihedral angle of 3.4°.

Single-crystal X-ray diffraction analyses reveal that complexes **1** and **2** are isostructural. The structure of **2** is similar to 1D polymer **1** only with Fe^{II} being substituted by Co^{II} (Fig.6) and slight differences in the bond distances and bond angles (Table 2). Such similar coordination polymers containing cationic chains of 4,4′-bpy as found in isostructural **1** and **2** have been reported[26-27], but the counter ion or the

Table 3 Hydrogen bond distances (nm) and bond angles (°) for polymers 1, 2 and 3

D–H⋯A	*d*(D-H)	*d*(H⋯A)	*d*(D⋯A)	∠(DHA)
1				
N4–H4⋯$O4^{iii}$	0.088 0	0.206 0	0.272 5(3)	131.1
O1–H1i⋯$O3^{iv}$	0.083 0	0.192 0	0.273 9(3)	172.2
O1–H1ii⋯$O5^{v}$	0.095 0	0.184 0	0.272 9(3)	155.9
O2–H2ii⋯$O4^{vii}$	0.081 0	0.190 0	0.269 8(3)	169.0
O2–H2i⋯$N5^{vi}$	0.107 0	0.173 0	0.279 9(4)	172.2
2				
N4–H4⋯$O4^{iii}$	0.092 0	0.199 0	0.270 6(3)	133.2
O1–H1ii⋯$O4^{iv}$	0.084 0	0.186 0	0.269 6(2)	174.4
O1–H1i⋯$N5^{v}$	0.075 0	0.204 0	0.278 0(3)	174.0
O2–H2i⋯$O3^{vi}$	0.082 0	0.193 0	0.274 9(2)	174.9
O2–H2ii⋯$O5^{vii}$	0.074 0	0.200 0	0.272 6(2)	167.9
3				
O7–H7i⋯O9	0.085 8(10)	0.194 0(3)	0.272 5(5)	152(5)
O7–H7ii⋯$O3^{vi}$	0.086 0(10)	0.188 1(19)	0.271 3(5)	163(5)
O8–8i⋯$O7^{vii}$	0.085 7(10)	0.203 9(13)	0.289 2(5)	174(5)
O8–H8ii⋯$O4^{iv}$	0.085 5(10)	0.187 6(16)	0.271 0(4)	165(4)

Symmetry code: **1**: ^{i} –*x*+1, *y*, –*z*+1/2; ^{ii} –*x*+3/2, –*y*+1/2, –*z*; ^{iii} –*x*+2, *y*, –*z*+1/2; ^{iv} –*x*+3/2, –*y*+1/2, –*z*+1; ^{v} –*x*+3/2, *y*–1/2, –*z*+1/2; ^{vi} *x*–1/2, *y*+1/2, *z*; ^{vii} *x*–1/2, –*y*+1/2, *z*–1/2. **2**: ^{i} –*x*+1, *y*, –*z*+1/2; ^{ii} –*x*+3/2, –*y*+1/2, –*z*; ^{iii} –*x*+2, *y*, –*z*+1/2; ^{iv} –*x*+3/2, –*y*+1/2, –*z*+1; ^{v} –*x*+3/2, *y*+1/2, –*z*+1/2; ^{vi} *x*–1/2, –*y*+1/2, *z*–1/2; ^{vii} *x*–1/2, *y*–1/2, *z*. **3**: ^{i} *x*, –*y*, *z*–1/2; ^{ii} –*x*, –*y*+1, –*z*; ^{iv} –*x*, –*y*, –*z*; ^{vi} –*x*+1/2, –*y*+1/2, –*z*; ^{vii} –*x*, *y*, –*z*–1/2.

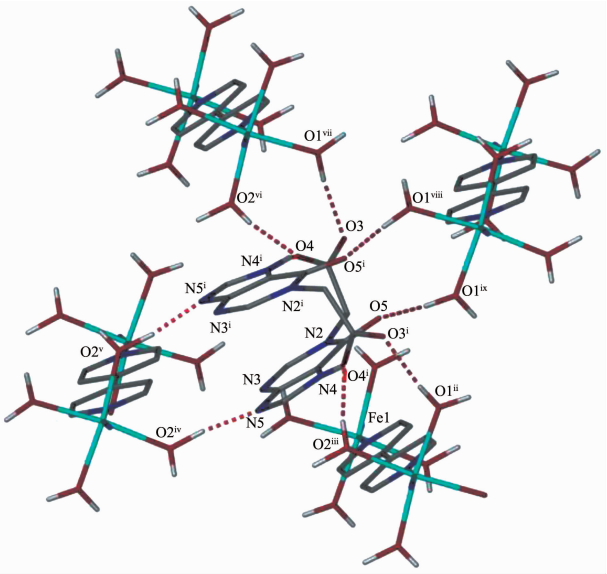

Symmetry code: [i] $-x+1, y, -z+1/2$; [ii] $-x+3/2, -y+1/2, -z$; [iii] $-x+2, y, -z+1/2$; [iv] $-x+3/2, -y+1/2, -z+1$; [v] $-x+3/2, y-1/2, -z+1/2$; [vi] $x-1/2, y+1/2, z$; [vii] $x-1/2, -y+1/2, z-1/2$

Fig.3　View of the hydrogen-bonding network in **1** showing the hydrogen-bonding occurrence between the coordinated water molecules and every dimeric anion $[(L')^-]_2$

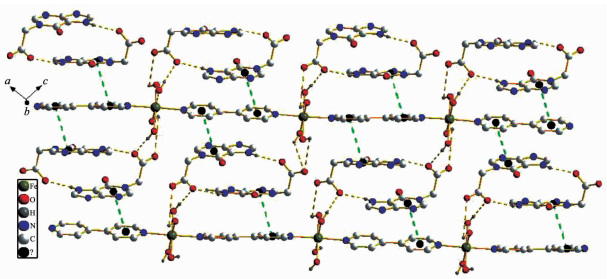

Hydrogen atoms are omitted for clarity

Fig.4　Drawing of the 2D framework in **1** formed by hydrogen bonds and π-π interactions between dimeric anions $[(L')^-]_2$ and 1D cationic chains

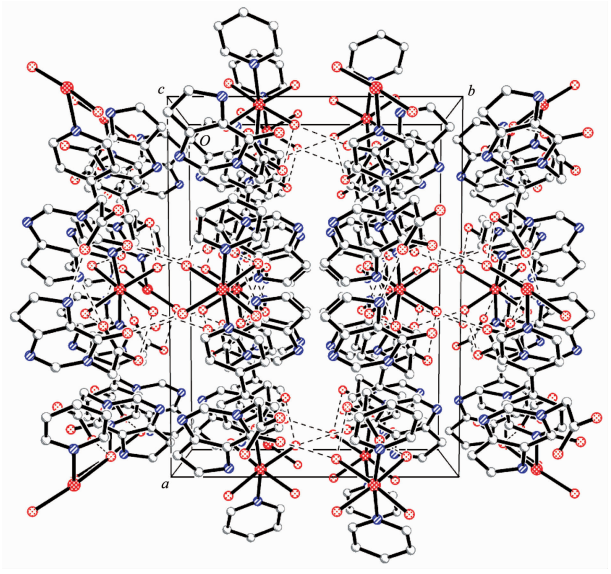

Hydrogen atoms are omitted for clarity

Fig.5　View of the 3D supramolecular network of **1**

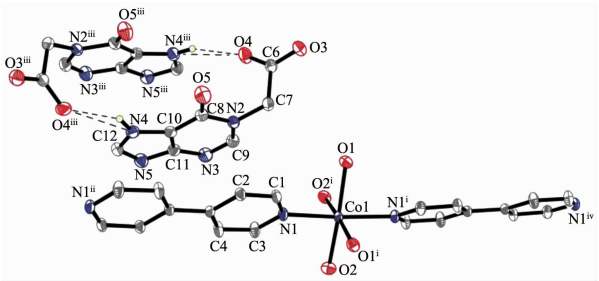

Counter ion of hydrogen-bonded cyclic dimmer $[(L')^-]_2$ with partial hydrogen atoms are omitted for clarity; Symmetry code: [i] $-x+1, y, -z+1/2$; [ii] $-x+3/2, -y+1/2, -z$; [iii] $2-x, y, -z+1/2$; [iv] $x-1/2, -y+1/2, z+1/2$

Fig.6　View of the coordination environment of the center Co^{Ⅱ} in **2** with thermal ellipsoids shown at 30% probability level

central atom is not the same as **1** and **2**.

2.2.2　Crystal structures of **3**

Complex **3** crystallizes in the monoclinic space group *C*2/*c*, and the overall structure of **3** is a 2D coordination polymer. The coordination environment of Eu^{Ⅲ} is shown in Fig.7, and the selected bond lengths and angles are given in Table 2. In **3**, two Eu^{Ⅲ} are connected together by oxalate produced by the decomposition of HL to form a dimeric unit, and the succinates bridge the dimeric units into a novel 2D polymer. The asymmetric unit of **3** contains one Eu^{Ⅲ}, one succinate, one-half oxalate, two coordinated water molecules, and one lattice water molecule. As shown in Fig.7, the central ion Eu^{Ⅲ} is coordinated by nine oxygen atoms with five oxygen atoms (O3, O4, O5^{iii}, O6^{iii}, and O6^{i}) from three succinates, two oxygen atoms (O1 and O2^{ii}) from one oxalate and two oxygen atoms (O7 and O8) from two coordinated water molecules. The bond lengths of nine EuO are in a range of 0.239 6(2) ~0.265 5(3) nm (Table 2). In **3** every oxalate acting as a bis(bidentate) ligand chelates with two Eu^{Ⅲ} ions, and each succinate adopts a μ_3-bridge mode with one carboxylate connecting two Eu^{Ⅲ} in a tridentate-chelating-bridging mode and the other carboxylate

coordinating to the third Eu$^{\text{Ⅲ}}$ in a bidentate-chelating mode. As a result, the oxalate-bridged dimeric units extend along *b* axis through the linkages of the tridentate-chelating-bridging carboxyl of succinates to form linear chains which are doubly bound up and down by succinates to produce a 2D layer as shown in Fig.8. The distance of Eu…Eu separated by oxalate is 0.629 1 nm whereas the distances of Eu…Eu separated by succinate are 0.421 0 nm and 0.647 7 nm.

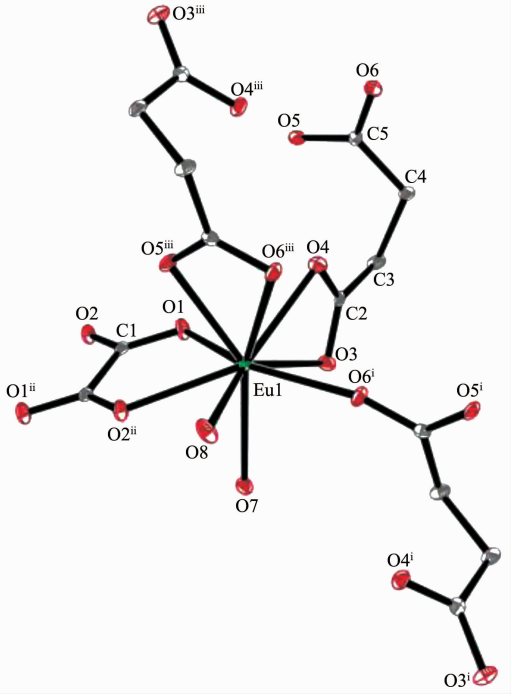

Hydrogen atoms are omitted for clarity; Symmetry code: [i] *x*, −*y*, *z*−1/2; [ii] −*x*, −*y*+1, −*z*; [iii] −*x*, *y*, −*z*+1/2

Fig.7 Coordination environment of the Eu$^{\text{Ⅲ}}$ in **3** with thermal ellipsoids shown at 30% probability level

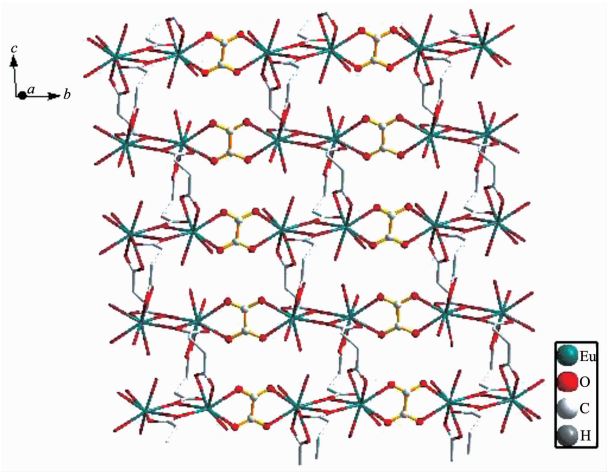

Hydrogen atoms are omitted for clarity

Fig.8 Drawing of the 2D framework in **3**

In **3**, there is a complicated hydrogen bond network, too (Table 3). There are two-sorted intralayer hydrogen bonds: one exists between the coordinated water O8 and the oxygen atom O4 of bidentate-chelating carboxyl of succinate from adjacent unit with O…O being 0.271 0(4) nm, and the other exists between coordinated water O8 and coordinated water O7 from adjacent unit with O…O being 0.289 2(5) nm. Besides, there are also two-sorted interlayer hydrogen bonds: one occurs from the coordinated water O7 to the oxygen atom O3 of the bidentate-chelating carboxyl of succinate from adjacent layer with O…O being 0.271 3(5) nm, and the other occurs from the coordinated water O7 to the lattice water O9 with O…O being 0.272 5(5) nm. Those two-sorted interlayer hydrogen bonds connect those 2D layers into a 3D supramolecular structure in **3** (Fig.9).

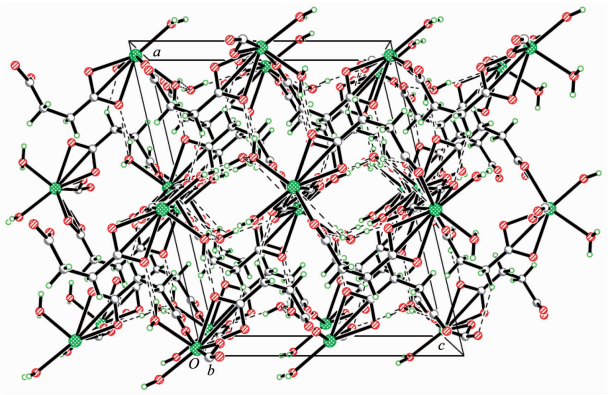

Fig.9 View of 3D supramolecular network of **3**

As discussed above, isostructural polymers **1** and **2** feature a 1D cationic chain and polymer **3** is a carboxylate-bridged 2D framework. The three complexes propagate into metal-organic supramolecular architectures by the aid of various kinds of intermolecular interactions such as hydrogen bonding, π-π stacking, Van der Waals force and so on. The hydrogen bonds are the main forces to hold the complex molecules together and sustain the crystal framework while the π-π interactions normally play important roles to direct the stacking fashion[28]. The chains of **1** and **2** are connected to form a 3D supramolecular framework by five-sorted hydrogen bonds while the 2D sheets of **3** extend into a 3D

supramolecular structure via two-sorted interlayer hydrogen bonds. The π-π stacking interactions (in **1** and **2**) and the two-sorted intralayer hydrogen bonds (in **3**) made the 3D supermolecule frameworks of these complexes more stable.

2.3 Thermal stability analysis of polymers 1 and 2

Thermogravimetric (TG-DSC) analysis was performed on polycrystalline samples for **1** and **2**, and the results are shown in (Fig.10). For **1**, there are three transitions in the decomposition. The first transition starts at 170 ℃ and ends at 216 ℃ with an endothermic peak at 180 ℃ with the loss of four coordinated water molecules (Obsd. 11.4%; Calcd. 11.0%). The second transition from 318 ℃ to 400 ℃ (30.0%) containing an endothermic peak at 353 ℃ is related to the loss of a deprotonated ligand L (Calcd. 28.2%). The third transition from 463 to 560 ℃ is related to the loss of the other deprotonated ligand L and the fragments of 4,4′-bpy molecule (Obsd. 43.7%; Calcd. 40.5%) with a strong exothermic peak at 543.3 ℃. The remaining residual at 800 ℃ is 14.9%, which agrees with the theoretical value (13.4%) calcu-lated by taking Fe_2O_3 as the final product. As shown in Fig. 10(b), the stability of polymer **2** is not similar to that of **1** although they are isostructural. Two transitions appear in the decomposition process of **2**. The first transition from 167.0 to 296.0 ℃ with an endothermic peak at 216.0 ℃ with a weight loss of 33.9% is related to the loss of four coordinated water molecules and one 4,4′-bpy molecule (Calcd. 34.8%). Two deprotonated ligands L are completely removed up to 548.5 ℃ containing a strong exothermic peak at 508.0 ℃, with the second weight loss of 54.3% corresponding to the result of the calculation of 56.2%. The remaining residue of 12.0% is supposed to be CoO (Calcd. 11.5%)[29-30].

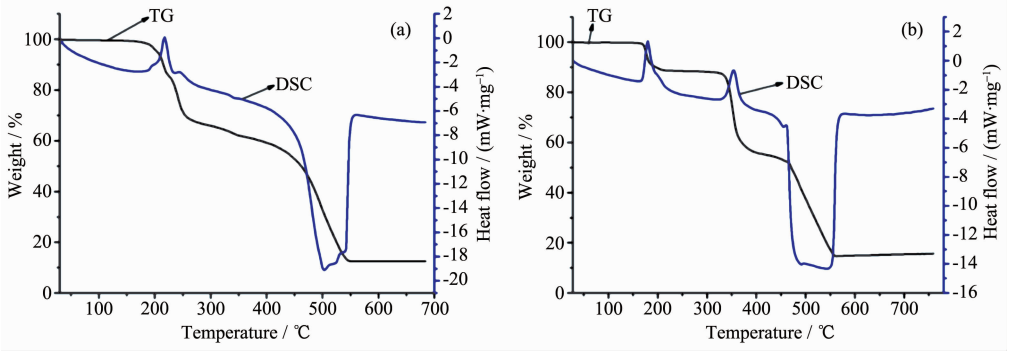

Fig.10　TG-DSC curves of **1** (a), and **2** (b)

2.4 Luminescence property of 3

We have measured the photoluminescence spectrum of solid sample of **3** at room temperature upon photo-excitation at 393 nm. As shown in Fig.11, there are two spectral bands at emission wavelengths *ca.* 590 nm and 613 nm which correspond to the $^5D_0 \rightarrow {}^7F_1$ and $^5D_0 \rightarrow {}^7F_2$ electronic transitions of the Eu Ⅲ ion, respectively.

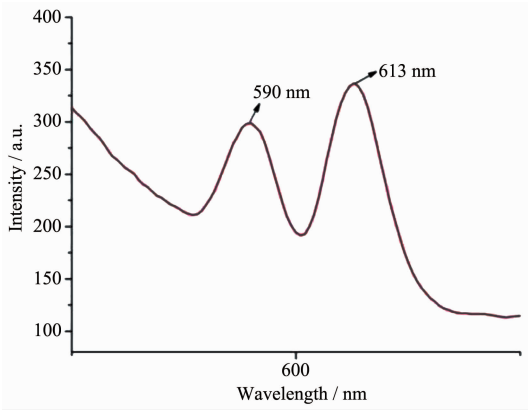

Fig.11　Emission spectrum of **3**

3 Conclusions

A purine-containing multifunctional ligand (HL) and three new coordination polymers **1**, **2** and **3** were synthesized and studied, respectively. Polymers **1** and **2** are isostructural and feature a 1D structure while **3** is a 2D polymer. In the three polymers, the deprotonated ligands L′ did not coordinated with central atom Fe Ⅱ, Co Ⅱ and Eu Ⅲ unlike the bridge

coordination of its tautomer HL in the literature[3], which indicates that the coordination ability of tautomer HL′ is not good. Interestingly, the hydrogen bonds are the main forces to hold the subunits together and sustain the crystal framework, and the π-π interactions normally play important roles to stabilize the resulting 3D supramolecular frameworks.

References:

[1] Qin Z Q, Jennings M C, Puddephatt R J. *Inorg. Chem.*, **2003**,**42**:1956-1965

[2] Wu J, Pan F F, Hou H W, et al. *Inorg. Chem. Commun.*, **2009**,**12**:750-754

[3] Liu X Q, Li Z Y, Yuan X J, et al. *J. Coord. Chem.*, **2012**,**65**:3721-3730

[4] García-Giménez J L, González-álvarez M, Liu-González M, et al. *J. Inorg. Biochem.*, **2009**,**103**:923-934

[5] Davis J T. *Angew. Chem. Int. Ed.*, **2004**,**43**:668-698

[6] Amo-Ochoa P, Castillo O, Alexandre S S, et al. *Inorg. Chem.*, **2009**,**48**:7931-7936

[7] Bishop A, Buzko O, Heyeck-Dumas S, et al. *Annu. Rev. Biophys. Biomol. Struct.*, **2000**,**29**:577-606

[8] Choquesillo-Lazarte D, Brandi-Blanco M P, García-Santos I, et al. *Coord. Chem. Rev.*, **2007**,**252**:1241-1256

[9] Cejudo R, Alzuet G, González-álvarez M, et al. *J. Inorg. Biochem.*, **2006**,**100**:70-79

[10]González-álvarez M, Alzuet G, Borrás J, et al. *J. Biol. Inorg. Chem.*, **2008**,**13**:1249-1265

[11]CUI Feng-Ling (崔凤灵), YAN Ying-Hua(闫迎华), ZHANG Qiang-Zhai(张强斋), et al. *Chemical Reagents*(化学试剂), **2008**,**30**(8):584-586

[12]CUI Feng-Ling (崔凤灵), XING Wei-Wei(邢卫卫), JIANG Xiao-Ying(江晓莹), et al. *Chinese J. Anal. Chem.*(分析化学), **2011**,**39**(5):728-732

[13]Das B, Baruah J B. *Cryst. Growth Des.*, **2011**,**11**:278-286

[14]Dubler E, Hanggi G, Schmalle H. *Acta Crystallogr., Sect. C*: *Cryst. Struct. Commun.*, **1987**,**43**:1872-1875

[15]Dubler E, Hanggi G, Bensch W. *J. Inorg. Biochem.*, **1987**, **29**:269-288

[16]Okabe N, Tsujita M. *Acta Crystallogr., Sect. C*: *Cryst. Struct. Commun.*, **2000**,**56**:1418-1419

[17]Mahata P, Prabu M, Natarajan S. *Cryst. Growth Des.*, **2009**, **9**:3683-3691

[18]Chen S S, Fan J, Okamura T, et al. *Cryst. Growth Des.*, **2010**,**10**:812-822

[19]Buglyó P, Crans D C, Nagy E M, et al. *Inorg. Chem.*, **2005**, **44**:5416-5427

[20]Liu Y L, Kravtsov V, Walsh R D, et al. *Chem. Commun.*, **2004**,**24**:2806-2807

[21]Bu X H, Tong M L, Xie Y B, et al. *Inorg. Chem.*, **2005**,**44**: 9837-9846

[22]Guo Z G, Li X J, Gao S Y, et al. *J. Mol. Struct.*, **2007**,**846**: 123-127

[23]Mao H Y, Zhang C Z, Li G. *Dalton Trans.*, **2004**,**22**:3918-3925

[24]Sheldrick G M. *SHELX*-97, *Program for the Solution and Refinement of Crystal Structures*, University of Göttingen, Germany, **1997**.

[25]Wu L, Yu Y H, Yuan X J, et al. *J. Coord. Chem.*, **2011**,**64**: 2804-2814

[26]Williams P A M , Ferrer E G, Baran E J, et al. *J. Argent. Chem. Soc.*, **2002**,**90**:109-115

[27]YANG Ying-Qun (杨颖群), LI Xu-Hong(李昶红), LI Wei(李薇), et al. *Chinese J. Inorg. Chem.*(无机化学学报), **2007**,**23**(10):1789-1792

[28]Li X P, Pan M, Zheng S R. *Cryst. Growth Des.*, **2007**,**7**:2481-2490

[29]Nadeem M A, Bhadbhade M, Bircher R, et al. *Cryst. Growth Des.*, **2010**,**10**:4060-4067

[30]Zeng M H, Zou H H, Hu S, et al. *Cryst. Growth Des.*, **2009**, **9**:4239-4242